JOURNAL OF AGRICULTURAL AND FOOD CHEMISTRY

J. Agric. Food Chem. **2008,** *56,* 9215–9224 **9215**

Kinetic Characterization of the Enzymatic and Chemical Oxidation of the Catechins in Green Tea

J. L. MUNOZ-MUNOZ,[†] F. GARCÍA-MOLINA,[†] M. MOLINA-ALARCÓN,[‡] J. TUDELA,[†] F. GARCÍA-CÁNOVAS,*[,†] AND J. N. RODRÍGUEZ-LÓPEZ[†]

GENZ, Grupo de Investigación de Enzimología, Departamento de Bioquímica y Biología Molecular-A, Facultad de Biología, Universidad de Murcia, E-30100 Espinardo, Murcia, Spain; and Departamento de Enfermería, Escuela Universitaria de Enfermería, Universidad de Castilla la Mancha, E-02071, Albacete, Spain

The oxidation of green tea catechins by polyphenol oxidase/O_2 and peroxidase/H_2O_2 gives rise to *o*-quinones and semiquinones, respectively, which inestability, until now, have hindered the kinetic characterization of enzymatic oxidation of the catechins. To overcome this problem, ascorbic acid (AH_2) was used as a coupled reagent, either measuring the disappearance of AH_2 or using a chronometric method in which the time necessary for a fixed quantity of AH_2 to be consumed was measured. In this way, it was possible to determine the kinetic constants characterizing the action of polyphenol oxidase and peroxidase toward these substrates. From the results obtained, (−) epicatechin was seen to be the best substrate for both enzymes with the OH group of the C ring in the cis position with respect to the B ring. The next best was (+) catechin with the OH group of the C ring in the trans position with respect to the B ring. Epigallocatechin, which should be in first place because of the presence of three vecinal hydroxyls in its structure (B ring), is not because of the steric hindrance resulting from the hydroxyl in the cis position in the C ring. The epicatechin gallate and epigallocatechin gallate are very poor substrates due to the presence of sterified gallic acid in the OH group of the C ring. In addition, the production of H_2O_2 in the auto-oxidation of the catechins by O_2 was seen to be very low for (−) epicatechin and (+) catechin. However, its production from the *o*-quinones generated by oxidation with periodate was greater, underlining the importance of the evolution of the *o*-quinones in this process. When the $[substrate]_0/[IO_4^-]_0$ ratio = 1 or ≫1, H_2O_2 formation increases in cases of (−) epicatechin and (+) catechin and practically is not affected in cases involving epicatechin gallate, epigallocatechin, or epigallocatechin gallate. Moreover, the antioxidant power is greater for the gallates of green tea, probably because of the greater number of hydroxyl groups in its structure capable of sequestering and neutralizing free radicals. Therefore, we kinetically characterized the action of polyphenol oxidase and peroxidase on green tea catechins. Furthermore, the formation of H_2O_2 during the auto-oxidation of these compounds and during the evolution of their *o*-quinones is studied.

KEYWORDS: Polyphenol oxidase; peroxidase; catechins; green tea; hydrogen peroxide

INTRODUCTION

Polyphenol oxidase (tyrosinase) (monophenol, *o*-diphenol; oxygen-oxidoreductase; EC 1.14.18.1; PPO) is a binuclear copper-cluster ubiquituously present in biological systems (*1, 2*). It catalyzes the oxidation of *o*-diphenols (*o*-diphenolase or catecholase activity) to the corresponding *o*-quinones, through the consumption of molecular oxygen. It may also catalyze the regioselective ortho-hydroxylation of monophenols to catechols (monophenolase or cresolase activity) and their subsequent oxidation to *o*-quinones. The resulting *o*-quinones may undergo nonenzymatic autopolymerisation to produce colored compounds (*3–5*). Browning in plant materials is associated with the enzymatic oxidation of phenolic compounds (*6, 7*).

Peroxidases are ubiquituous in the fungi, plant, and animal kingdoms (*8*).The cationic isoenzyme from horseradish peroxidase (EC 1.11.1.7; POD) has been studied intensively because of its commercial use in diagnostic assays and potential application in bioremediation (*9*). The oxidation of phenols by POD produces extremely reactive free radical intermediates, which following release from the enzyme, readily condense to yield polymeric products of variable stoichiometry. Because of this, the kinetics of these reactions were not described by classical Michaelis−Menten equations for a long time before a suitable method was found, which permitted the typical

* To whom correspondence should be addressed. Fax: +34 968 364147. E-mail: canovasf@um.es.

[†] Universidad de Murcia.

[‡] Universidad de Castilla la Mancha.

10.1021/jf8012162 CCC: $40.75
Published on Web 09/13/2008

Scheme 1

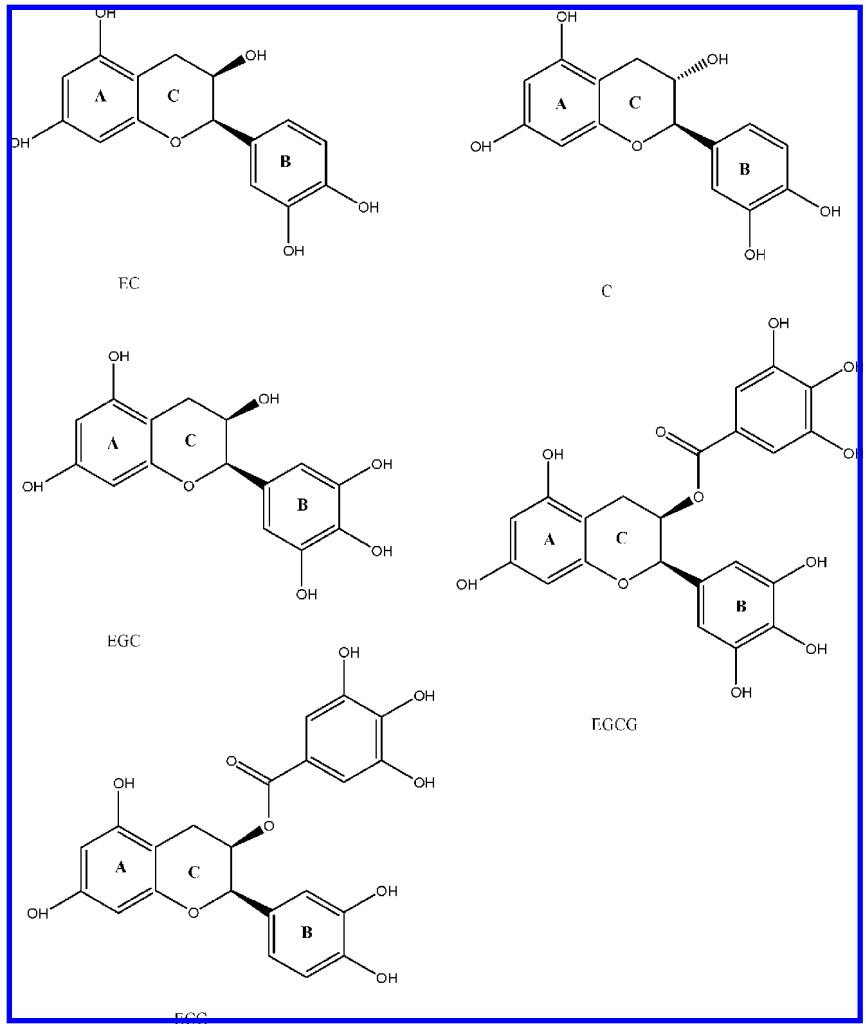

Michaelis−Menten kinetics to be established with a series of *o*-diphenols, monophenols, and anilines (*9–11*).

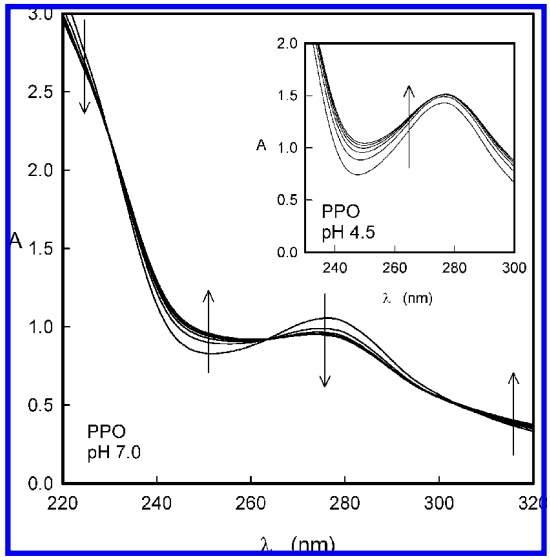

Figure 1. Spectrophotometric scans of the evolution of *o*-quinone, Q, generated with a high concentration of PPO. Experimental conditions were 30 mM phosphate buffer pH 7.0, $[ECG]_0 = 0.1$ mM, $[E]_0 = 60$ nM; scans were made every 60 s. **Inset**: Experimental conditions were 30 mM acetate buffer pH 4.5, $[ECG]_0 = 0.1$ mM, $[E]_0 = 60$ nM; scans were made every 60 s.

Tea is a popular beverage all over the world. The growing evidence of the potential health benefits of tea has prompted a large number of investigations into tea, its major components, and their biological activities. The overall results indicate that every type of tea (green, black, white, dark, yellow, and oolong) have significant antimutagenic and anticlastogenic effects (*12*). Additionally, tea catechins and their gallate esters possess antioxidant properties that prevent lipid peroxidation in erythrocyte membranes and microsomes and suppress the mutagenic effects induced by H_2O_2 (*12*). Tea extracts and individual tea polyphenols display both antioxidant and pro-oxidant effects (*13*). On the one hand, tea has been known for a long time to help prevent many diseases including cardiovascular diseases and cancer. The last claim is commonly attributed to the pronounced antioxidant activity of tea polyphenols. On the other hand, tea polyphenols have been reported as cytotoxic and mutagenic agents. This may be associated with the pro-oxidant activity of tea polyphenols as a result of their tendency to autoxidation accompanied by the formation of active forms of oxygen (reactive oxygen species, ROS) (*13*). We have recently demonstrated the inhibition of the dihydrofolate reductase enzyme, by the components of green tea (*14–16*).

Although the autoxidation of tea polyphenols has received substantial attention in the literature (*17*), the kinetic characterization of the enzymes involved in the transformation of these polyphenols, PPO and POD, is rather limited. It has been proposed that both enzymes participate in the browning and

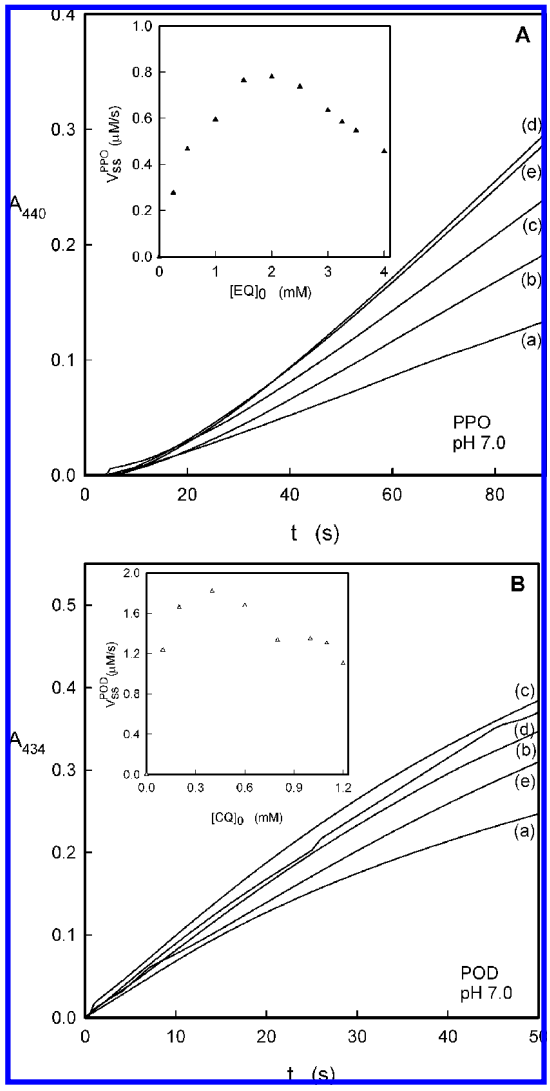

Figure 2. Spectrophotometric recordings of Q generated in the action of PPO and POD on (**A**) EC and (**B**) C. (**A**) Experimental conditions were 30 mM sodium phosphate pH 7.0, $\lambda = 440$ nm, $[PPO]_0 = 0.56$ nM. The substrate concentrations were (a) 0.5 mM, (b) 1 mM, (c) 1.5 mM, (d) 2 mM, and (e) 2.5 mM. **Inset**: Initial slope, V_0 vs $[EC]_0$, directly measuring the appearance of Q. (**B**) Experimental conditions were 30 mM sodium phosphate buffer pH 7.0, $\lambda = 440$ nm, $[POD]_0 = 9.1$ nM, and $[H_2O_2]_0 = 150$ μM. The substrate concentrations were (a) 0.1 mM, (b) 0.2 mM, (c) 0.4 mM, (d) 0.6 mM, and (e) 0.8 mM. **Inset**: Initial slope, V_0 vs $[C]_0$, directly measuring the appearance of Q.

spoilage of fruits and vegetables (*18, 19*). The formation of products resulting from the evolution of the *o*-quinones and semiquinones originated by the action of purified strawberry PPO and POD has been studied (*18*). Recently, considerable attention has been given to the possible inhibition displayed by green tea catechins, especially on melanin biosynthesis (*20*). It has been suggested that they act on PPO, thus playing a role in the regulation of this biosynthetic route (*20*). In addition, the formation of H_2O_2 in green tea as a result of autoxidation of its components has been studied (*21–25*), and its possible physiological function in plant tissues has been discussed (*23*).

The instability of the products originated by the action of PPO and POD (*o*-quinones and semiquinones, respectively) is responsible for the formation of H_2O_2 and at the same time hinders the kinetic characterization of these substrates (*9, 26*). For this reason, we used ascorbic acid (AH_2) to prevent the evolution of these products and characterized the enzymes by two spectrophotometric

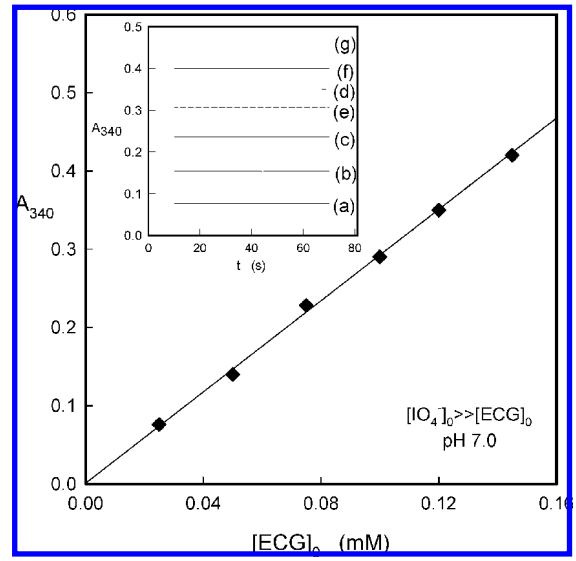

Figure 3. Determination of the molar absorptivity of the *o*-quinone of EGC. Plot of Absorbance vs $[S]_0$. Absorbance values at $\lambda = 340$ nm obtained by oxidation with excess periodate. The experimental conditions were 30 mM sodium phosphate buffer pH 7.0. The concentration of IO_4^- was 0.5 mM, and $[EGC]_0$ was (a) 0.025 mM, (b) 0.05 mM, (c) 0.075 mM, (d) 0.1 mM, (e) 0.12 mM, (f) 0.145 mM, and (g) 0.17 mM. **Inset**: Kinetics of the evolution of Q generated with excess of periodate.

Table 1. Molar Absorptivities of the *o*-Quinones of the Catechins[a]

	$\varepsilon^{4.5}$ (M^{-1} cm^{-1})		$\varepsilon^{7.0}$ (M^{-1} cm^{-1})	
substrate	λ_{max}	λ_i	λ_{max}	λ_i
C	4184 ± 210		4800 ± 288	3125 ± 125
EC	4900 ± 340		5482 ± 250	
EGCG	8800 ± 440	450 ± 22	8995 ± 360	650 ± 30
EGC	32000 ± 1600	4500 ± 325	3829 ± 153	21000 ± 1050
ECG	13357 ± 800	15100 ± 906	9300 ± 370	5102 ± 200

[a] The oxidation was carried out at ratios $[IO_4^-]_0/[\text{catechins}]_0 \gg 1$ at pHs 4.5 and 7.0. The maximum wavelengths (λ_{max}) for the *o*-quinones were determined. Some *o*-quinones showed a constant absorbance at a determined wavelength, isosbestic point (λ_i). The molar absorptivities at a specified pH value ($\varepsilon^{4.5}$ and $\varepsilon^{7.0}$) were determined at the corresponding λ_{max} and λ_i, as described in **Figure 3**.

methods, either measuring the disappearance of AH_2 or using a chronometric method in which the time necessary for a fixed quantity of AH_2 to be consumed was measured. At the same time, H_2O_2 formation (pro-oxidant capacity) was studied from two different viewpoints along with the antioxidant potential of the products. Particular attention was paid to green tea and its major constituents, (−) epicatechin (EC), (+) catechin (C), epigallocatechin (EGC), epicatechin gallate (ECG), and epigallocatechin gallate (EGCG) (**Scheme 1**).

MATERIALS AND METHODS

Reagents. Mushroom polyphenol oxidase (PPO; 1530 U mg^{-1}), horseradish peroxidase (POD; 251 U mg^{-1}), catalase (9300 U mg^{-1}), and superoxide dismutase (SOD; 4140 U mg^{-1}) were obtained from Sigma Chemical (St. Louis, MO). PPO was purified as described elsewhere (*26*). POD was purchased from Sigma (type VI; Rz = 3.2) and used without further purification. The concentration of POD was determined spectrophotometrically using a Soret molar absorptivity of 102 mM^{-1} cm^{-1} (*9*). The protein concentration was determined by the Bradford's method (*27*) and using bovine serum albumin as the standard. (−) Epicatechin (EC), (+) catechin (C), (−) epicatechin gallate (ECG), (−) epigallocatechin (EGC), (−) epigallocatechin gallate (EGCG), and 2,2′-azino-bis(3-ethylbenzothiazoline-6-sulfonic acid) (ABTS) were obtained from Sigma Chemical (St. Louis, MO), and sodium periodate was obtained from Scharlau (Malaga, Spain). Stock solutions of the reducing substrates were

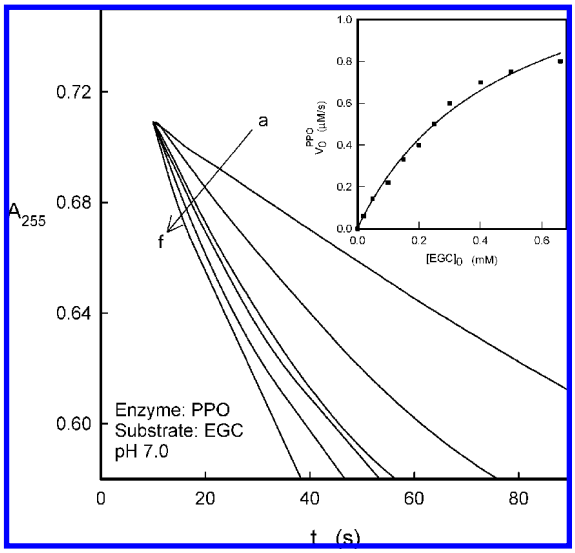

Figure 4. AH_2 disappearance method for characterizing the enzymatic activity of PPO on EGC. Experimental conditions were 30 mM sodium phosphate buffer pH 7.0, $\lambda = 255$ nm, $[E]_0 = 2$ nM, and $[AH_2]_0 = 20$ μM. Substrate concentrations were (a) 0.05 mM, (b) 0.075 mM, (c) 0.1 mM, (d) 0.15 mM, (e) 0.2 mM, and (f) 0.3 mM. **Inset**: Plot of V_0^{PPO} true steady-state rate vs $[EGC]_0$.

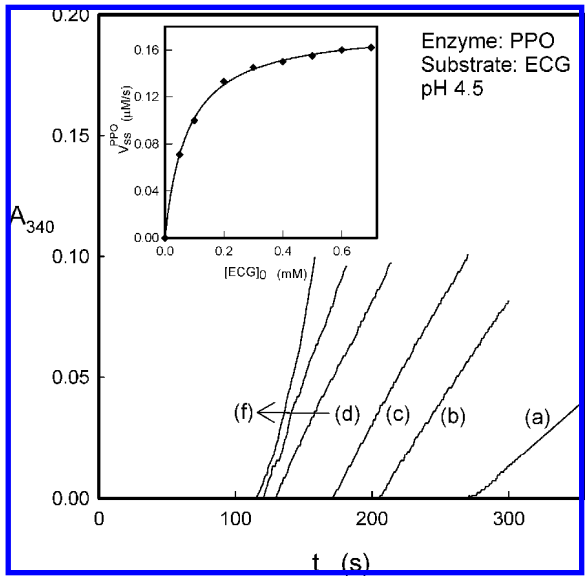

Figure 5. Chronometric method for characterizing the enzymatic activity of PPO on ECG. Experimental conditions were 30 mM sodium acetate buffer pH 4.5, $\lambda = 340$ nm, $[E]_0 = 4.2$ nM, and $[AH_2]_0 = 20$ μM. Substrate concentrations were (a) 0.05 mM, (b) 0.1 mM, (c) 0.2 mM, (d) 0.3 mM, (e) 0.4 mM, and (f) 0.6 mM. **Inset**: Plot of V_0^{PPO} vs $[ECG]_0$.

Scheme 2

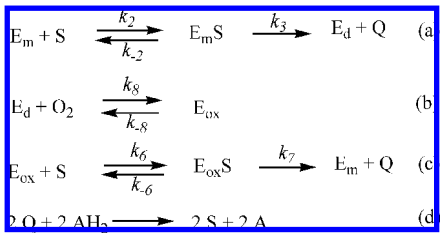

prepared in 0.15 mM phosphoric acid to prevent auto-oxidation. The buffers used were 30 mM sodium phosphate buffer (pH 7.0) and 30 mM sodium acetate (pH 4.5).

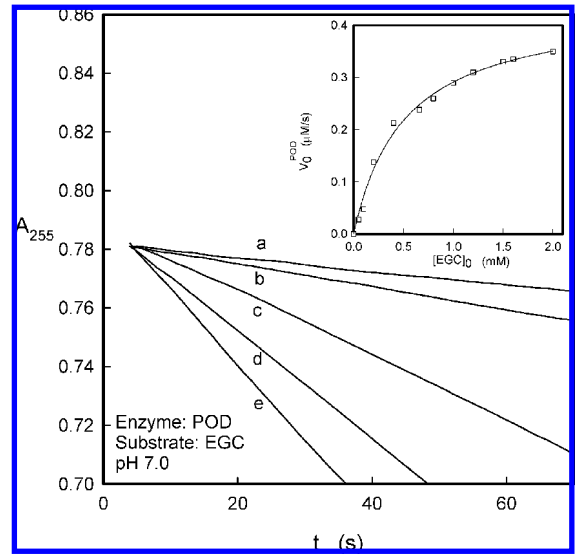

Figure 6. AH_2 disappearance method for characterizing the enzymatic activity of POD on EGC. Experimental conditions were 30 mM sodium phosphate buffer pH 7.0, $\lambda = 255$ nm, $[E]_0 = 1.76$ nM, $[AH_2]_0 = 20$ μM, and $[H_2O_2]_0 = 200$ μM. Substrate concentrations were (a) 0.05 mM, (b) 0.1 mM, (c) 0.2 mM, (d) 0.4 mM, and (e) 0.66 mM. **Inset**: Plot of V_0^{POD} vs $[EGC]_0$.

Scheme 3

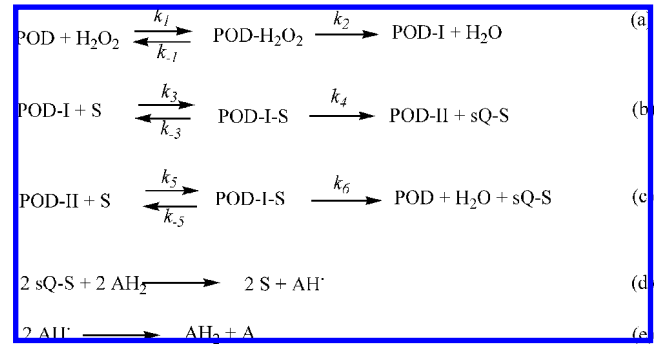

Spectrophotometric Assays. Absorption spectra were recorded in a visible−ultraviolet Perkin-Elmer Lambda 35 spectrophotometer interfaced online with a PC compatible Intel-Pentium microcomputer, at a scanning speed of 60 nm/s controlled by the UV-Winlab software. The temperature was maintained at 25 °C using a Haake D16 circulating water bath with a heater/cooler and checked using a Cole-Parmer digital thermometer with a precision of 0.1 °C. Kinetic assays were also carried out with the above instruments following the disappearance of AH_2 at $\lambda = 255$ nm ($\varepsilon = 7970$ M^{-1} cm^{-1}) or using a chronometric method (detailed below). Reference cuvettes contained all the components, except the substrate and AH_2, in a final volume of 1 mL. All the assays were carried out with PPO saturated by molecular oxygen (0.26 mM in the assay medium) (*28*) or with POD saturated by H_2O_2 (*9*).

Oxymetric Assays. Oxygen evolution was measured with a Clark-type electrode coupled to a Hansatech Oxygraph (King's Lynn, Norfolk, U.K.). The equipment was calibrated using the tyrosinase/4-*tert*-butylcatechol method (*29*). Nitrogen was bubbled through the reaction medium to remove the oxygen when necessary. The reaction medium contained 30 mM sodium phosphate buffer, pH 7.0. The medium was stirred constantly, and the temperature was kept at 25 ± 0.1 °C using a Haake D1G circulating water-bath.

Chronometric Method. Enzymatic activity was determined spectrophotometrically using the chronometric method described in the Results and Discussion section (*9, 30, 31*). The only condition was that there had to be an absorbance increase (due to the product formation) measurable once the ascorbic acid (AH_2) was consumed to be able to determine the time necessary, τ, to consume the quantity of AH_2 called $[AH_2]_0$. From these values, the initial rate, V_0, can be

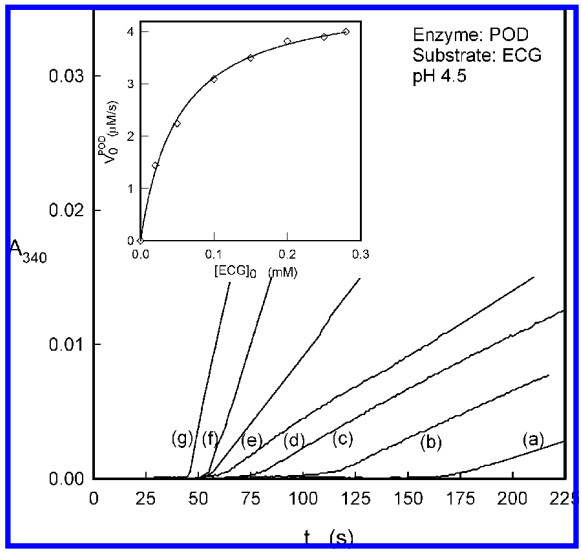

Figure 7. Chronometric method for characterizing the enzymatic activity of POD on ECG. Experimental conditions were 30 mM sodium acetate buffer pH 4.5, $\lambda = 340$ nm, $[E]_0 = 52$ nM, $[AH_2]_0 = 65$ μM, and $[H_2O_2]_0 = 200$ μM. Substrate concentrations were (a) 0.025 mM, (b) 0.05 mM, (c) 0.1 mM, (d) 0.15 mM, (e) 0.2 mM, (f) 0.25 mM, and (g) 0.28 mM. **Inset**: Plot of V_0^{POD} vs $[ECG]_0$.

Scheme 4

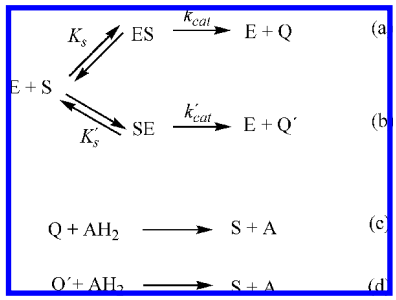

determined (see the Results and Discussion section). Preliminary experiments were carried out in the absence of ascorbic acid with the tyrosinase/O_2/catechin system by recording spectrophotometric scans to identify in which zone of the spectrum, particularly the visible zone, the greatest changes in absorbance occurred. The wavelength chosen at acid and neutral pH was 330 nm. The activity of POD was continued using the same methodology but with the POD/H_2O_2/catechin system.

Determination of the *o*-Quinone Molar Absorptivities. The absorbance data were analyzed according to Beer's law using the standard least-squares linear regression program. Molar absorptivities were estimated for a known path length of 1 cm. The minimal acceptable coefficient of correlation (R) was taken to be 0.995. Data yielding coefficients less than this were due to pipetting errors and rounding up/down of the values. With this precaution, the 95% confidence limits for the molar absorptivity estimates were ≤5%.

Determination of H_2O_2 Generated. *1. Auto-oxidation of Catechins.* (a) Oxymetric experiment. The auto-oxidation of each of the catechins of green tea was followed by measuring oxygen consumption in an oxygraph in 30 mM phosphate buffer, pH 7.0. After 60 min, 0.2 μM of catalase was added, and the instantaneous appearance of oxygen was measured according to the following stoichiometry: $2\ H_2O_2 \rightarrow O_2 + 2\ H_2O$.

(b) Spectrophotometric experiments. The catechins were preincubated in 30 mM phosphate buffer, pH 7.0. After 60 min, the unoxidised catechins and the quinones were extracted twice with ether at pH 4.5. The H_2O_2 generated was evaluated in an aliquot of aqueous extract using the POD/ABTS system at $\lambda = 414$ nm, measuring the $ABTS^{\bullet+}$ radical ($\varepsilon = 31\ 100\ M^{-1}\ cm^{-1}$) in 0.1 M acetate buffer, pH 4.5 (*9*).

Table 2. Kinetic Constants for PPO and POD at Both pH Values[a]

PPO					
substrate	method	k_{cat}^{PPO} (s^{-1})	K_m^{PPO} (mM)	K_m^{O2} (μM)	$k_6 \times 10^5$ ($M^{-1}\ s^{-1}$)
			pH 4.5		
C	τ_{440}	335 ± 32.1	0.41 ± 0.13	14.50 ± 0.13	8.2 ± 0.40
EC	τ_{440}	696 ± 68.5	0.55 ± 0.17	30.20 ± 0.41	12.6 ± 0.50
EGCG	τ_{320}	33 ± 3.3	0.50 ± 0.06	1.43 ± 0.13	0.6 ± 0.03
EGC	A_{255}	18 ± 2.1	0.30 ± 0.04	0.78 ± 0.09	0.6 ± 0.04
ECG	τ_{340}	15 ± 0.8	0.16 ± 0.02	0.65 ± 0.03	0.9 ± 0.05
			pH 7.0		
C	τ_{440}	355 ± 31.2	0.38 ± 0.11	15.40 ± 0.15	9.34 ± 0.40
EC	τ_{440}	706 ± 70.2	0.51 ± 0.14	30.70 ± 0.50	14.01 ± 0.50
EGCG	τ_{320}	40 ± 3.9	0.45 ± 0.05	1.73 ± 0.13	0.88 ± 0.03
EGC	A_{255}	23 ± 2.8	0.50 ± 0.02	1.00 ± 0.10	0.46 ± 0.04
ECG	τ_{340}	21 ± 1.9	0.11 ± 0.03	0.91 ± 0.11	1.91 ± 0.05

POD					
substrate	method	k_{cat}^{POD} (s^{-1})	K_m^{POD} (mM)	K_m^{H2O2} (μM)	$k_5 \times 10^6$ ($M^{-1}\ s^{-1}$)
			pH 4.5		
C	τ_{440}	1995 ± 120	0.71 ± 0.11	117 ± 7.02	2.81 ± 0.27
EC	τ_{440}	2080 ± 153	0.23 ± 0.04	122 ± 8.54	9.04 ± 0.61
EGCG	τ_{320}	1900 ± 76	0.16 ± 0.03	112 ± 7.84	11.87 ± 0.59
EGC	A_{255}	430 ± 25	0.53 ± 0.08	25 ± 1.02	0.81 ± 0.06
ECG	τ_{340}	680 ± 70	0.05 ± 0.01	40 ± 2.27	13.60 ± 0.65
			pH 7.0		
C	τ_{440}	2065 ± 103	0.75 ± 0.15	122 ± 6.10	2.75 ± 0.15
EC	τ_{440}	2166 ± 160	0.25 ± 0.05	127 ± 7.62	8.66 ± 0.41
EGCG	τ_{320}	1963 ± 137	0.21 ± 0.02	115 ± 8.05	9.35 ± 0.69
EGC	A_{255}	425 ± 21	0.51 ± 0.06	25 ± 1.47	0.83 ± 0.07
ECG	τ_{340}	700 ± 49	0.07 ± 0.01	41 ± 2.81	10.00 ± 0.86

[a] τ_λ = Chronometric method at wavelength λ. A_λ = Disappearance of AH2 at wavelength λ.

Table 3. Rate of Oxygen Consumption and Production of Oxygen during the Oxidation of Catechins by Molecular Oxygen[a]

	$V_0^{O2} \times 10^3$ (μM/min)		$[H_2O_2]$ (μM)	
	−SOD[b]	+SOD[c]	catalase[d]	POD/ABTS[e]
EC	5.1 ± 0.2	1.1 ± 0.1		1.82 ± 0.12
C	5.3 ± 0.2	1.2 ± 0.1		1.33 ± 0.06
ECG	253.1 ± 7.6	124.2 ± 6.2	16 ± 1	17.51 ± 0.71
EGCG	375.3 ± 9.8	301.3 ± 9.9	14 ± 1	15.82 ± 0.47
EGC	492.2 ± 9.9	159.1 ± 6.5	16 ± 1	16.11 ± 0.64

[a] Substrate concentration was always 0.1 mM at pH 7.0. [b] Absence of superoxide dismutase. [c] Presence of superoxide dismutase (414 units). [d] $[H_2O_2]$ determination with the addition of catalase (930 units). [e] $[H_2O_2]$ determination with the POD/ABTS method.

2. Oxidation of Catechins with Periodate. (a) Stoichiometric oxidation of catechins with periodate. Oxidation of the catechins in 30 mM phosphate buffer pH 7.0 was carried out with stoichiometric periodate. The mixture was acidified to pH 4.5, and the *o*-quinones generated were extracted twice with ether. Then, the *o*-quinones were extracted from the ether phase with 30 mM phosphate buffer pH 7.0 and allowed to evolve for 60 min, after which following acidification to pH 4.5, the *o*-quinones, dimers, and trimers formed were extracted with ether. The H_2O_2 generated in an aliquot of the aqueous extract was evaluated by the POD/ABTS system at $\lambda = 414$ nm, measuring the $ABTS^{\bullet+}$ radical in acetate buffer 0.1 M, pH 4.5.

(b) Oxidation of catechins by periodate in defect. The catechins were oxidized in a 5/1 defect ratio, following the same procedure as in section 2 (a).

Kinetic Data Analysis. For PPO, the initial rate values (V_0^{PPO}) were calculated from triplicate measurements at each reducing substrate concentration $[S]_0$, and V_0^{PPO} versus $[S]_0$ data were adjusted to the Michaelis−Menten equation (eq 6) through the Sigma Plot 9.0 program

Table 4. Production of H_2O_2 during Evolution of the *o*-Quinones Generated by Oxidation with Periodate

	$[S]_0/[IO_4^-]_0$[a] (mM/mM)	$[H_2O_2]$[c] (μM)	$[S]_0/[IO_4^-]_0$[b] (mM/mM)	$[H_2O_2]$[c] (μM)	EC50[d]	ARP[e]	n[f]
EC	0.1/0.1	80 ± 4	0.5/0.1	200.1 ± 10	0.16	6.25	3.12
C	0.1/0.1	78 ± 3	0.5/0.1	180.1 ± 9	0.18	5.55	2.77
ECG	0.1/0.1	20 ± 1	0.5/0.1	40.2 ± 2	0.03	32.26	16.67
EGCG	0.1/0.1	19 ± 1	0.5/0.1	38.1 ± 2	0.06	16.67	8.33
EGC	0.1/0.1	18 ± 1	0.5/0.1	36.5 ± 2	0.11	9.09	4.54

[a] $[S]_0/[IO_4^-]_0 = 1$. [b] $[S]_0/[IO_4^-]_0 = 5$. [c] $[H_2O_2]$ was determined using the POD/ABTS method. [d] EC50 = ratio of the antioxidant concentration necessary to decrease the initial concentration of $ABTS^{\bullet-}$ to 50%. [e] ARP = antiradical power (1/EC50). [f] n = stoichiometric number of electrons of $ABTS^{\bullet-}$ involved in the reaction with each antioxidant (1/(2EC50)).

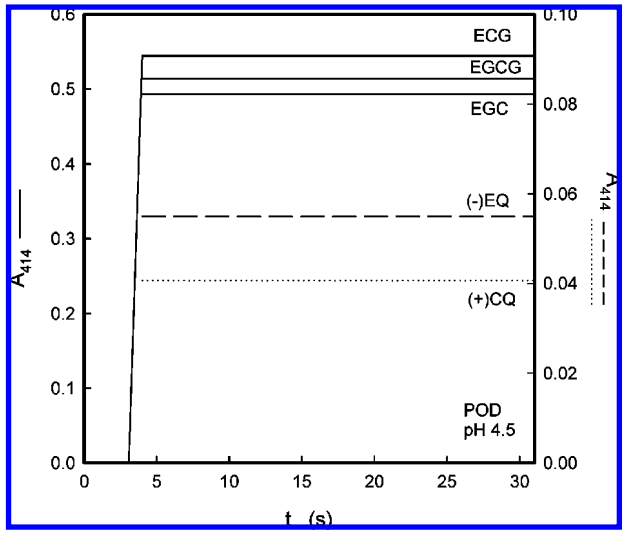

Figure 8. Spectrophotometric quantification of H_2O_2 generated during the auto-oxidation of different green tea catechins. The method described in the Materials and Methods section was followed. Initial concentration of all the substrates was 0.1 mM, and the experimental conditions were $[ABTS]_0 = 5$ mM, $[POD]_0 = 0.22$ μM, and 30 mM sodium acetate buffer pH 4.5. The increase in absorbance due to the formation of $ABTS^{\bullet+}$ was measured at 414 nm for (a) C, (b) EC, (c) EGC, (d) EGCG, and (e) ECG.

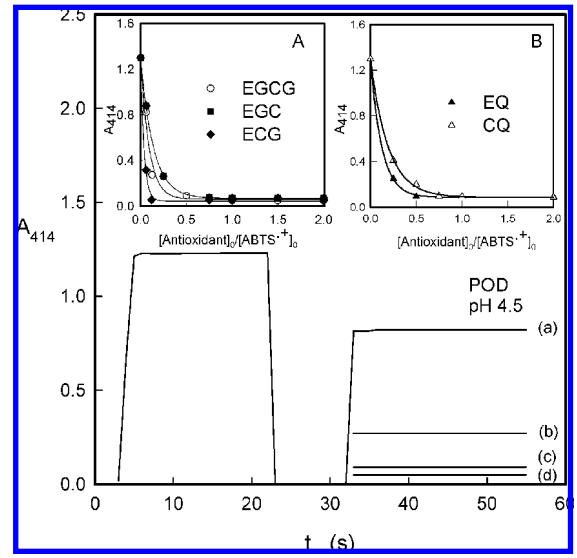

Figure 9. Evaluation of antioxidant activity. Disappearance of absorbance of $ABTS^{\bullet+}$ with time at 414 nm when different quantities of EGCG were added to pregenerated quantities of $ABTS^{\bullet+}$ (40 μM). Experimental conditions were 30 mM sodium acetate buffer pH 4.5, $\lambda = 414$ nm, $[POD]_0 = 0.22$ μM, $[ABTS]_0 = 5$ mM, and $[H_2O_2]_0 = 20$ μM, and the substrate concentrations were (a) 2.4 μM, (b) 5 μM, (c) 30 μM, and (d) 80 μM. The substrates were (a) EGC, (b) ECG, (c) EGCG, (d) EC, and (e) C. **Insets**: (**A**) The disappearance of $ABTS^{\bullet+}$ as a function of the $[antioxidant]_0/[ABTS^{\bullet+}]_0$ at 414 nm; the substrates were (○) EGCG, (■) EGC, and (◆) ECG. (**B**) The disappearance of $ABTS^{\bullet+}$ as a function of the $[antioxidant]_0/[ABTS^{\bullet+}]_0$ at 414 nm; the substrates were (▲) EC and (△) C.

for Windows (*32*), obtaining the maximum rate (V_{max}^{PPO}) and Michaelis constant for the substrate (K_m^{PPO}). From these values and according to eq 7, one can calculate the catalytic constant (k_{cat}^{PPO}). Knowing the value of k_8 (the binding constant of oxygen to the *deoxy*-tyrosinase form (E_d)), the value of the Michaelis constant for O_2 (K_m^{O2}) can be obtained following eq 9 (*26*). For POD, the initial rate values (V_0^{POD}) were calculated from triplicate measurements at each reducing substrate concentration, and V_0^{POD} versus $[S]_0$ data were fitted to the Michaelis−Menten equation (eq 11) through the Sigma Plot 9.0 program for Windows (*32*), obtaining V_{max}^{POD} and K_m^{POD}. From these values and according to eqs 12 and 14, and knowing k_1 (*9*), one can calculate k_{cat}^{POD} (eq 12) and the Michaelis constant for H_2O_2 ($K_m^{H2}O2$) (eq 14).

RESULTS AND DISCUSSION

Oxidation of Green Tea Catechins by High Concentrations of PPO. To characterize the green tea catechins as substrates of PPO and POD, the stability of the *o*-quinones generated in the oxidation step was first studied, by carrying out oxidation experiments using PPO (**Figure 1**). The enzymatic oxidation of EGC by PPO at pH 7.0 generates *o*-quinone (Q), which is unstable and evolves with a very clear stoichiometry, as revealed by the formation of three isosbestic points at 230, 265, and 310 nm (**Figure 1**), which are not maintained at high substrate concentrations. In similar experiments carried out at pH 4.5, no isosbestic points were produced because the *o*-quinone did not follow a clearly defined stoichiometry (**Figure 1**, **inset**). The instability of the *o*-quinones means that these measurements could not be considered reliable for kinetically characterizing the enzymes. This was confirmed in the experiments depicted in **Figure 2A** and **B** showing the oxidation of catechin by PPO/O_2 and POD/H_2O_2. The representations of V_0 versus $[S]_0$ point to an apparent inhibition caused by the excess of substrate, so that this method is of no use for the kinetic characterization of these enzymes and other experimental methods must be used (see below).

Oxidation of Green Tea Catechins by Excess of Periodate. Periodate oxidizes *o*-diphenols in a way similar to PPO, but when an excess of periodate is used for the oxidation, the reaction is instantaneous. The *o*-quinone generated is more stable, and this allowed the molar absorptivities to be calculated for Q at pH 7.0 and pH 4.5 (**Figure 3**) (*33*). These values are shown in **Table 1**. This physical characteristic of Q is important in several types of study, such as those involving HPLC or for determining the concentration of Q.

Kinetic Characterization of the Oxidation of Green Tea Catechins by PPO and POD. As mentioned above, the kinetic characterization of green tea catechins cannot be carried out by measuring the formation of *o*-quinones due to their instability.

However, a spectrophotometric method using a reductant such as AH_2, which instantaneously reduces Q to S, thus preventing its chemical evolution, can be used by following the disappearance of AH_2 (**Figure 4** and **Figure 4**, **inset**) or by measuring the time necessary for a fixed quantity of the reductant to be consumed (chronometric method) (*9, 30, 31*) (**Figure 5**, **inset**).

In the case of PPO, reactions **a**−**c** of **Scheme 2** correspond to the enzymatic catalysis (*34*) and reaction **d** to the reduction of Q to S by AH_2. V_0^{PPO}, the steady-state rate, corresponds to the disappearance rate of AH_2 (**Figure 4**). Nonlinear regression fitting of V_0^{PPO} versus $[S]_0$ according to eq 6 (**Figure 4**, **inset**) gives K_m^{PPO} and V_{max}^{PPO}. In **Scheme 2**, E_m, E_d, and E_{ox} represent the oxidized and deoxygenated forms and that with a peroxide group of the enzyme, respectively.

In the case of POD, the activity can also be followed by measuring the disappearance of AH_2 (**Figure 6** and **Figure 6**, **inset**). The action of POD on reducing substrates (S) in the presence of AH_2 is described by **Scheme 3** (*9*), where POD corresponds to free enzyme, POD-I to compound I, POD-II to compound II, and sQ-S is the semiquinone radical corresponding to S.

Figure 6 depicts the action of POD on EGC, measuring the disappearance of AH_2. Note the difference in the reduction stoichiometry of the products of both enzymes. In PPO reaction **d** (**Scheme 2**), the reduction is $1AH_2/1Q$. However, in POD reactions **d** and **e** (**Scheme 3**), the stoichiometry is $1AH_2/2SQ$-S. In the first case, then, the real steady-state rate V_0^{PPO} is measured and in the second $V_0^{POD}/2$.

The spectrophotometric method described above does not serve to characterize all substrates because the spectra of AH_2 and some catechins overlap, so that a chronometric method is necessary based on measuring the time needed for a small quantity of AH_2 to be consumed (*9, 30, 31*).

Deduction of the Steady-State Rate Expression by the Chronometric Method. The expression of V_0 as a function of AH_2 is derived by applying the material balance method. It is assumed that enzymatic reactions rapidly reach the steady state (when $t \rightarrow 0$), so that the steady-state rate of the enzyme is V_0. The products of both reactions (**Schemes 2** and **3**) react with AH_2, consuming it at the same time, so that the concentration remaining at time t is

$$[AH_2]_t = [AH_2]_0 - V_0 t \quad (1)$$

where the term $V_0 t$ is the matter generated by the enzyme (PPO or POD).

When no AH_2 remains, the following will be true at time $t = \tau$:

$$0 = [AH_2]_0 - V_0 \tau \quad (2)$$

and so

$$V_0^{PPO} = \frac{[AH_2]_0}{\tau} \quad (3)$$

Therefore, if we can experimentally determine τ, then, knowing $[AH_2]_0$, V_0^{PPO} can be calculated according to eq 3; τ can be experimentally determined if a spectrophotometric signal indicates that AH_2 has been consumed (see **Figures 5** and **7**).

In the case of POD (**Scheme 4**), the expression of V_0 (eq 3) must be modified by taking into consideration the stoichiometry (steps **d** and **e**):

$$V_0^{POD} = \frac{2[AH_2]_0}{\tau} \quad (4)$$

This method was used to kinetically characterize EC, C, EGCG, and ECG as substrates of PPO and POD (**Table 2** and **Figures 5** and **7**).

The values of V_0 obtained by both of these methods were analyzed by nonlinear regression to the Michaelis equation.

The analytical expression of V_0^{PPO} in the case of PPO is (*34*)

$$V_0^{PPO} = \frac{V_{max}^{PPO}[S]_0[O_2]_0}{K_m^{PPO}K_S^{O_2} + K_m^{O_2}[S]_0 + K_m^{PPO}[O_2]_0 + [S]_0[O_2]_0} \quad (5)$$

The values of K_m^{O2} for PPO are very small (*35*), so that at the concentration of O_2 in the solution (0.26 mM), the enzyme is saturated and eq 5 is transformed into

$$V_0^{PPO} = \frac{V_{max}^{PPO}[S]_0}{K_m^{PPO} + [S]_0} \quad (6)$$

The values of K_m^{PPO} and V_{max}^{PPO} can be obtained from eq 6 and taking into account (*28*) that

$$V_{max}^{PPO} = 2k_{cat}^{PPO}[E]_0 \quad (7)$$

$$K_m^{PPO} = \frac{k_{cat}^{PPO}}{k_6} \quad (8)$$

$$K_m^{O_2} = \frac{k_{cat}^{PPO}}{k_8} \quad (9)$$

we can calculate k_{cat}^{PPO} and K_m^{O2} from eqs 7 and 9, respectively, since $k_8 = (2.3 \pm 0.4) \times 10^7\ M^{-1}\ s^{-1}$ (*28*). From eq 8, the kinetic constant for the binding of the substrate to E_{ox} (*28*) can be determinated. The values are shown in **Table 2**.

As regards POD, the kinetic analysis of the mechanism shown in **Scheme 3** (*9*), results in

$$V_0^{POD} = \frac{V_{max}^{POD}[S]_0[H_2O_2]_0}{K_m^{POD}[H_2O_2]_0 + K_m^{H_2O_2}[S]_0 + [S]_0[H_2O_2]_0} \quad (10)$$

at saturating concentrations of H_2O_2:

$$V_0^{POD} = \frac{V_{max}^{POD}[S]_0}{K_m^{POD} + [S]_0} \quad (11)$$

$$V_{max}^{POD} = 2k_{cat}^{POD}[E]_0 \quad (12)$$

$$K_m^{POD} = \frac{k_{cat}^{POD}}{k_5} \quad (13)$$

$$K_m^{H_2O_2} = \frac{k_{cat}^{POD}}{k_1} \quad (14)$$

The value of k_1 is $1.7 \times 10^7\ M^{-1}\ s^{-1}$ (*9*). From eq 12, we can calculate k_{cat}^{POD} and from eq 14, $K_m^{H2}O2$. The constant for the binding of the substrate to compound II can be calculated from eq 13. Therefore, the analysis of the data according to eqs 11 and 14 provides the kinetic information shown in **Table 2**.

For the substrates indicated in **Scheme 1**, the data obtained for the enzymatic oxidation are shown in **Table 2**, and they indicate that both enzymes show similar behavior. As regards C, similar values of K_m^{PPO} have been described for PPO from Indian tea leaves (*36*) and marula fruit (*37*) but much higher values in mushroom PPO in organic solvents (*38*). Note that the studies that describe the K_m^{PPO} for C do not provide the k_{cat}^{PPO} because the *o*-quinones evolve although it would be possible to obtain by measuring the consumption of oxygen. The best

substrate for both enzymes is EC, which has a diphenolic structure and between the B ring and the OH of the C ring is in the cis position; the values of K_m^{PPO} are within the same order of magnitude (**Table 2**). The order of catalysis of the different catechins with respect to PPO k_{cat}^{PPO} is EC > C > EGCG > EGC > ECG. However, in the case of POD, the order is EC > EGC > EGCG > C > ECG. The values of K_m^{O2} and K_m^{H2O2}, which depend on k_{cat}, (eqs 9 and 14), follow the same order as k_{cat} and are very low in all cases. In physiological conditions, then, these enzymes can catalyze the transformation of catechins at low concentrations of O_2 and H_2O_2.

As regards the data shown in **Table 2**, the low values of k_{cat} obtained for both enzymes with EGCG and ECG. In the gallate derivates (ECG and EGCG), the enzyme may act on the B ring, *o*-diphenol in ECG or pyrogallol in EGCG, or even on the gallate bound to the C ring. In the first case, k_{cat} should be high (particularly with EGCG) due to the three hydroxyls vecinal with respect to the *o*-diphenol of ECG (*26*). However, if the enzyme binds to the substrate through the gallate portion, the electron withdrawing effect will make k_{cat} much lower, as can be seen in **Scheme 4**.

In **Scheme 4**, S represents ECG or EGCG, the complex ES represents the binding to the B ring and the complex SE the binding to the gallate portion of the same molecule of substrate.

As the product in both cases is reduced by AH_2, the total activity is measured by the chronometric method (**Figures 5** and **7**), giving

$$V_{ss} = \frac{\left(\frac{k_{cat}K'_S + K'_{cat}K_S}{K_S + K'_S}\right)[S]_0[E]_0}{\frac{K_S K'_S}{K_S + K'_S}} \quad (15)$$

The Michaelis constant of PPO for free pyrogallol is high (*26*), $K_S = 1.96$ mM, while for gallic acid $K'_S = 0.20$ mM (unpublished data). Therefore, $K_S \gg K'_S$, $K'_S/K_S \ll 1$, and eq 15 can be expressed as

$$V_{ss} = \frac{\left(\frac{k_{cat}K'_S}{K_s} + K'_{cat}\right)[S]_0[E]_0}{K'_S + [S]_0} \quad (16)$$

with

$$K_m^{app} = K'_S \quad (17)$$

and

$$k_{cat}^{app} = \frac{k_{cat}K'_S}{K_S} + K'_{cat} \quad (18)$$

From eq. 16, it should be noted that these substrates, kinetically, should have a low K_m^{app} (K'_S) and low k_{cat}^{app} ($k_{cat} > k'_{cat}$). Data obtained experimentally with PPO support the reaction mechanism described in **Scheme 4**, since when the enzyme acts on free pyrogallol $k_{cat}^{PPO} = 1263\ s^{-1}$ (*28*) and on free gallic acid $k_{cat}^{PPO} = 27\ s^{-1}$ (unpublished data). Moreover, there should be steric hindrance because of the cis position between the gallate of the C ring and B ring. However, this is not reflected in the values of K_m^{app}, since k_{cat}^{app} in **Table 2** is low. K_m^{app} represents K_m (PPO) or (POD), respectively. k_{cat}^{app} represents k_{cat} (PPO) or (POD), respectively.

Production of H_2O_2. Catechins have been described as both antioxidants and pro-oxidants due to their capacity to scavenger free radicals and to form H_2O_2 (*13, 17*). In this work, we study the autoxidation of the catechins by measuring the oxygen consumption rate during the oxidation of the reduced substrates using an oxygraph. In these experiments, the effect of the enzyme superoxide dismutase (SOD) was observed, and the formation of H_2O_2 was followed by adding catalase (in the oxygraph) or spectrophotometrically at $\lambda = 414$ nm, using POD/ABTS.

(a) Oxygen consumption rate. The oxygen consumption rate increased with the concentration of both substrates, catechin and O_2 (results not shown). This result agrees with the findings of other authors (*13, 17*) and confirms that oxidation begins with the substrate reacting with O_2 (*5*). Thus, the oxygen consumption rate is very low for EC and C and higher for EGC, EGCG, and ECG (**Table 3**).

(b) Inhibition of oxygen consumption by superoxide dismutase. In all the substrates studied, SOD inhibited oxygen consumption, in agreement with (*13, 17*) (**Table 3**), indicating the formation of $O_2^{\bullet -}$ and its sequestering:

$$2O_2^{\bullet -} + 2H^+ \rightarrow O_2 + H_2O_2 \quad (19)$$

Furthermore, the presence of SOD diminishes H_2O_2 formation, since according to (*17*), the stoichiometry is $2O_2^{\bullet -}/1H_2O_2$, although the $O_2^{\bullet -}$ can also provoke the reaction of the reduced substrate with the superoxide anion and generating H_2O_2, where the stoichiometry is $1O_2^{\bullet -}/1H_2O_2$.

(c) Formation of H_2O_2. The formation of H_2O_2 in the autoxidation of some catechins has been demonstrated by several authors (*13, 17, 39, 40*). Here, we compare the formation of H_2O_2 during the autoxidation of C, EC, EGC, ECG, and EGCG at pH = 7.0. Its formation was measured by oxygraph from the activity of the enzyme catalase or after twice extracting the remaining substrate with ether and evaluating the H_2O_2 (**Figure 8**). Three situations have been considered: (*i*) Direct autoxidation. We refer to the formation of H_2O_2, which is accumulated in the medium through the direct oxidation by O_2 and by the $O_2^{\bullet -}$ generated. As can be seen in **Table 3**, the values of C and EC are low, while those obtained with ECG, EGC, and EGCG are relatively high; (*ii*) Oxidation with stoichiometric periodate. When the different catechins are oxidized with stoichiometric periodate, the results shown in **Table 4** point to the slight evolution of the *o*-quinones corresponding to ECG, EGC, and EGCG, while the *o*-quinones corresponding to C and EC lead to the formation of large quantities of H_2O_2. These results show how the *o*-quinones in C, EC, and ECG evolve to generate the highest values of H_2O_2 and also confirm that the limiting step is the reaction described in eq 19; (*iii*) Oxidation of catechins by defect periodate. These conditions are equivalent to those in the action of PPO on its substrates, during which *o*-quinones are generated that can react with the substrate again, as indicated in (*41–43*). **Table 4**shows the results obtained, evaluating H_2O_2 as described in the Materials and Methods. The evolution of the *o*-quinones of C and EC, as they react with the substrate and oxygen, leads to the formation of large quantities of H_2O_2. However, the *o*-quinones of ECG, EGC, and EGCG produce less H_2O_2.

Antioxidant Power. Besides quantifying the H_2O_2 formed during the autoxidation of each substrate, we assessed their antioxidant power using the POD/ABTS/ H_2O_2 system (*44, 45*). For this, the radical $ABTS^{\bullet +}$ is generated with a limiting hydrogen peroxide, while keeping the concentration of the radical constant. By varying the antioxidant, we calculate the EC50 (the concentration of antioxidant that lowers the concentration of radical by 50%) (see **Figure 9**) (*45*). In addition, we calculate the number of electrons of the radical involved in its reaction with each particular oxidant (n_{ABTS}). As can be seen, the gallates of green tea have a lower EC50 and therefore higher antiradical or antioxidant power

(ARP), defined as the inverse of the EC50 (*46, 47*). The catechins have a lower ARP; of the gallates, ECG has the highest antioxidant power. This work therefore demonstrates the dual effect of catechins and gallates from green tea as regards their pro- and antioxidant power in biological systems.

In conclusion, the use of a chronometric method with AH_2 and the measurement of the variation in absorbance of AH_2 with time, to determine the enzymatic activity of PPO and POD acting on green tea catechins, enabled the kinetic characterization of these compounds, which act as substrates for both enzymes. The catechins with a diphenolic structure, C and EC, are better substrates than the epigallocatechins, while among the catechins, the best is EC because of the cis position of the OH in the C ring. From the results obtained, we conclude that green tea catechins do not inhibit the melanogenesis pathway by acting on PPO, as has been claimed (*20*). Rather, these compounds act as an alternative to the physiological substrates L-tyrosine and L-DOPA. It seems therefore that catechins direct the melanogenesis pathway toward quinonic derivatives other than *o*-dopaquinone and dopachrome, which are intermediates of the melanogenesis pathway. However, their oxidation by PPO and POD contributes to the browning of tea and other vegetables that contain catechins (*19*). On the other hand, there has been extensive investigation into the ways by which tea catechins might act in cancer prevention. The observed pro-oxidant nature of these catechins appears to conflict with the generally recognized concept that tea polyphenolics act as antioxidants. Here, we demonstrate that tea catechins possess both antioxidant and pro-oxidant properties. However, and despite these properties, several investigations have suggested that tea polyphenols might act on different cellular targets such as the proteasome (*48*), 5-cytosine DNA methyltransferase (*49*), and dihydrofolate reductase (*14–16*), among others. Deciphering the mechanisms by which tea catechins affect several molecular and cellular pathways would be of importance for the rational use of these compounds in the prevention and treatment of cancer and other physiological disorders.

LITERATURE CITED

(1) Solomon, E. I.; Sundaran, U. M.; Machonkin, T. E. Multicopper oxidases and oxygenases. *Chem. Rev.* **1996**, *96*, 2563–2606.

(2) Klabunde, T.; Eicken, C.; Sacchettini, J. C.; Krebs, B. Crystal structure of a plant catechol oxidase containing a dicopper center. *Nat. Struct. Biol.* **1998**, *5*, 1084–1090.

(3) García-Carmona, F.; García-Canovas, F.; Iborra, J. L.; Lozano, J. A. Kinetic study of the pathway of melanization between L-dopa and dopachrome. *Biochim. Biophys. Acta* **1982**, *717*, 124–131.

(4) Garcia-Cánovas, F.; Garcia-Carmona, F.; Vera-Sanchez, J.; Iborra, J. L.; Lozano, J. A. The role of pH in the melanin biosynthesis pathway. *J. Biol. Chem.* **1982**, *257*, 8738–8744.

(5) Rodriguez-Lopez, J. N.; Tudela, J.; Varón, R.; Garcia-Canovas, F. Kinetic study on the effect of pH on the melanin biosynthesis pathway. *Biochim. Biophys. Acta* **1991**, *1076*, 379–386.

(6) Whitaker, C. Y.; Lee, Y. In *Enzymatic Browning and Its Prevention*; Whitaker, J. R., Lee C. Y., Eds.; American Chemical Society: Washington, DC, 1995.

(7) Walker J. R. L. In *Enzymatic Browning and Its Prevention*; Whitaker, J. R., Lee, C. Y., Eds.; American Chemical Society: Washington, DC, 1995.

(8) Dunford H. B. *Heme Peroxidases*; Wiley-VHC: New York, 1999; pp 92−97.

(9) Rodríguez-López, J. N.; Gilabert, M. A.; Tudela, J.; Thorneley, R. N. F.; García-Cánovas, F. Reactivity of horseradish peroxidase compound II toward substrates: kinetic evidence for a two-step mechanism. *Biochemistry* **2000**, *39*, 13201–13209.

(10) Gilabert, M. A.; Fenoll, L. G.; Garcia-Molina, F.; Tudela, J.; Garcia-Canovas, F.; Rodríguez-López, J. N. Kinetic characterization of phenol and anilines derivates as substrate of peroxidase. *Biol. Chem.* **2004**, *385*, 795800.

(11) Gilabert, M. A.; Hiner, A. N.; Garcia-Ruiz, P. A.; Tudela, J.; Garcia-Molina, F.; Acosta, M.; Garcia-Canovas, F.; Rodríguez-López, J. N. Differential substrate behaviour of phenol and aniline derivatives during oxidation by horseradish peroxidise: kinetic evidence for a two-step mechanism. *Biochim. Biophys. Acta* **2004**, *1699*, 235–243.

(12) You-Ying, T.; Xin-Qing, X.; Hui-Long, X.; Naoharu, W. Optimization of theaflavin biosynthesis from tea polyphenols using an inmobilized enzyme system and response surface methodology. *Biotechnol. Lett.* **2005**, *27*, 269–274.

(13) Roginsky, V.; Alegria, A. E. Oxidation of tea extracts and tea catechins by molecular oxygen. *J. Agric. Food Chem.* **2005**, *53*, 4529–4535.

(14) Navarro-Martinez, M. D.; Navarro-Peran, E.; Cabezas-Herrera, J.; Ruiz-Gomez, J.; Garcia-Canovas, F.; Rodriguez-Lopez, J. N. Antifolate activity of epigallocatechin gallate against *Stenophomonas maltophilia*. *Antimicrob. Agents Chemother.* **2005**, *49*, 2914–2920.

(15) Navarro-Peran, E.; Cabezas-Herrera, J.; Hiner, A. N. P.; Sadunishvili, T.; Garcia-Canovas, F.; Rodriguez-Lopez, J. N. Kinetics of the inhibition of bovine liver dihydrofolate reductase by tea catechins: origin of sowl-binding inhibition and pH studies. *Biochemistry* **2005**, *44*, 7512–7525.

(16) Navarro-Peran, E.; Cabezas-Herrera, J.; Garcia-Canovas, F.; Durrant, M. C.; Thorneley, R. N. F.; Rodriguez-Lopez, J. N. The antifolate activity of tea catechins. *Cancer Res.* **2005**, *65*, 2059–2064.

(17) Mochizuki, M.; Yamazaki, S. I.; Kano, K.; Ikeda, T. Kinetic analysis and mechanistic aspects of autooxidation of catechins. *Biochim. Biophys. Acta* **2002**, *1569*, 35–44.

(18) Lopez-Serrano, M.; Ros-Barcelo, A. Kinetic properties of (+)catechin oxidation by a basic peroxidase isoenzyme from strawberries. *J. Food Chem.* **1997**, *62*, 676–723.

(19) Lopez-Serrano, M.; Ros-Barcelo, A. Comparative study of the products of the peroxidase-catalyzed and the polyphenol oxidase-catalyzed (+)-catechin oxidation. Their possible implications in strawberry (*Fragaria* × *ananassa*) browning reactions. *J. Agric. Food Chem.* **2002**, *50*, 1218–1224.

(20) No, J. K.; Soung, D. Y.; Kim, Y. J.; Shim, K. H.; Jun, Y. S.; Rhee, S. H.; Yokozawa, T.; Chung, H. Y. Inhibition of tyrosinase by green tea components. *Pharmacol. Lett.* **1999**, *65*, 241–246.

(21) Chung, F. L.; Schwartz, J.; Herzog, C. R.; Yang, Y. M. Tea and cancer prevention: studies in animals and humans. *J. Nutr.* **2003**, *133*, 3268–3274.

(22) Chen, Z. Y.; Zhu, Q. Y.; Wong, Y. F.; Zhang, Z.; Chung, H. Y. Stabilizing effect of ascorbic acid on green tea catechins. *J. Agric. Food Chem.* **1998**, *46*, 2512–2516.

(23) Long, L. H.; Lan, A. N. B.; Hsuan, P. Y. Y.; Halliwell, B. Generation of hydrogen peroxide by "antioxidant" beverages and the effect of milk addition. Is cocoa the best beverage. *Free Radical Res.* **1999**, *31*, 65–71.

(24) Peng, M.; Kuc, J. Peroxidase-generated hydrogen-peroxide as a source of antifungal activity in vitro and on tobacco leaf-disks. *Phytopathology* **1992**, *82*, 696–699.

(25) Murray, R. D. H. *Progress in the Chemistry of Organic Natural Products*; Springer-Verlag: New York, 1999; pp 84−316.

(26) Rodríguez-Lopez, J. N.; Fenoll, L. G.; Garcia-Ruiz, P. A.; Varon, R.; Tudela, J.; Thorneley, R. N.; Garcia-Canovas, F. Stopped-flow and steady-state study of the diphenolase activity of mushroom tyrosinase. *Biochemistry* **2000**, *39*, 10497–10506.

(27) Bradford, M. M. A rapid and sensitive method for the quantitation of microgram quantities of protein utilizing the principle of protein-dye binding. *Anal. Biochem.* **1976**, *72*, 248–254.

(28) Rodríguez-Lopez, J. N.; Ros, J. R.; Varon, R.; GarciaCanovas, F. Oxygen Michaelis constant for tyrosinase. *Biochem. J.* **1993**, *293*, 859–866.

(29) Rodriguez-Lopez, J. N.; Ros-Martinez, J. R.; Varon, R.; Garcia-Canovas, F. Calibration of a Clark-type oxygen electrode by tyrosinase-catalyzed oxidation of a 4-*tert*-butylcatechol. *Anal. Biochem.* **1992**, *202*, 356–360.
(30) Muñoz, J. L.; Garcia-Molina, F.; Varon, R.; Rodríguez-Lopez, J. N.; Garcia-Canovas, F.; Tudela, J. Calculating molar absortivities for quinones: application to the measurements of tyrosinase activity. *Anal. Biochem.* **2006**, *351*, 128–138.
(31) Garcia-Molina, F.; Munoz, J. L.; Varon, R.; Rodríguez-Lopez, J. N.; Garcia-Canovas, F.; Tudela, J. A review on spectrophotometric methods for a measuring the monophenolase and diphenolase activities of tyrosinase. *J. Agric. Food Chem.* **2007**, *55*, 9739–9749.
(32) Jandel Scientific. SigmaPlot 9 for Windows; Jandel Scientific: Core Madera, CA, 2007.
(33) Weidman, S. W. A kinetic study of the periodate oxidation of catechol. *J. Am. Chem. Soc.* **1966**, *88*, 5820–5827.
(34) Sanchez-Ferrer, A.; Rodriguez-Lopez, J. N.; Garcia-Canovas, F.; Garcia- Carmona, F. Tyrosinase: A conprehensive review of its mechanism. *Biochim. Biophys. Acta* **1995**, *1247*, 1–11.
(35) Fenoll, L. G.; Rodrigez-Lopez, J. N.; Garcia-Molina, F.; Garcia-Canovas, F.; Tudela, J. Michaelis constant of mushroom tyrosinase with respect to oxygen in the presence of monophenols and diphenols. *Int. J. Biochem. Cell Biol.* **2002**, *34*, 332–336.
(36) Halder, J.; Tamuli, P.; Bhaduri, A. N. Isolation and characterization of polyphenol oxidase from Indian tea leaf (*Camellia sinensis*). *J. Nutr. Biochem.* **1998**, *9*, 75–80.
(37) Mdluli, K. M. Partial purification and characterisation of polyphenol oxidase and peroxidase from marula fruit (*Sclerocarya birrea* subsp. *Caffra*). *Food Chem.* **2005**, *92*, 311–323.
(38) Kermasha, S.; Bao, H.; Bisakowski, B. Biocatalysis of tyrosinase using catechin assubstrate in selected organic solvent media. *J. Mol. Catal. B: Enzym.* **2001**, *11*, 292–238.
(39) Jiang, Y.; Miles, P. W. Generation of H_2O_2 during enzymic oxidation of catechin. *Phytochemistry* **1993**, *33*, 29–34.
(40) Akagawa, M.; Shigemitsu, T.; Suyama, K. Production of hydrogen peroxide by polyphenols and polyphenol-rich beverages under quasi-physiological conditions. *Biosci. Biotechnol. Biochem.* **2003**, *67*, 2632–2640.
(41) Jimenez-Atiénzar, M.; Cabanes, J.; GandiaHerrero, F.; Garcia-Carmona, F. Kinetic analysis of catechin oxidation by polyphenol oxidase at neutral pH. *Biochem. Biophys. Res. Commun.* **2004**, *319*, 902–910.
(42) Guyot, S.; Vercauteren, J.; Cheynier, V. Structural determination of colourless and Bellow Diners resulting from (+)-catechin coupling catalysed by grape polyphenol oxidase. *Phytochemistry* **1996**, *42*, 1279–1288.
(43) Guyot, S.; Cheynier, V.; Souquet, J. M.; Moutounet, M. Influence of pH on the enzymatic oxidation of (+)-catechin in model systems. *J. Agric. Food Chem.* **1995**, *43*, 2458–2462.
(44) Cano, A.; Hernandez-Ruiz, J.; Garcia-Canovas, F.; Acosta, M.; Arnao, M. B. An end-point method for estimation of the total antioxidant activity in plant material. *Phytochem. Anal.* **1998**, *9*, 196–202.
(45) Hotta, H.; Nagano, S.; Ueda, M.; Tsujino, Y.; Koyama, J.; Osakai, T. Higher radical scavenging activities of polyphenolic antioxidants can be ascribed to chemicals reactions following their oxidation. *Biochem. Biophys. Acta* **2002**, *1572*, 123–132.
(46) Torres, J. L.; Lozano, C.; Maher, P. Conjugation of catechins with cysteine generates antioxidant compounds with enhanced neuroprotective activity. *Phytochemistry* **2005**, *66*, 2032–2037.
(47) Brand-Williams, W.; Cuvelier, M. E.; Berset, C. Use of a free radical method to evaluate antioxidant activity. *Lebensm.−Wiss. Technol.* **1995**, *28*, 25–30.
(48) Nam, S.; Smith, D. M.; Dou, Q. P. Ester bond-containing tea polyphenols potently inhibit proteasome activity in vitro and in vivo. *J. Biol. Chem.* **2001**, *276*, 13322–13330.
(49) Fang, M. Z.; Wang, Y.; Ai, N.; Hou, Z.; Sun, Y.; Lu, H.; Welsh, W.; Yang, C. S. Tea polyphenol (−)-epigallocatechin-3-gallate inhibits DNA methyltransferase and reactivates methylation-silenced genes in cancer cell lines. *Cancer Res.* **2003**, *63*, 7563–7570.

Received for review April 17, 2008. Revised manuscript received July 1, 2008. Accepted July 2, 2008. This paper has been partially supported by grants from the Ministerio de Educación y Ciencia (Madrid, Spain) Project BIO2006-15363 and SAF2006-07040-C02-01, from the Fundación Séneca (CARM, Murcia, Spain) Project 00672/PI/04, and from the Consejería de Educación (CARM, Murcia, Spain) BIO-BMC 06/01-0004. J.L.M.-M. has a fellowship from the Ministerio de Educación y Ciencia (Madrid, Spain) Reference AP2005-4721. F.G.-M. has a fellowship from Fundación Caja Murcia (Murcia, Spain).

JF8012162